University of Baghdad
College of Engineering
JOURNAL OF ENGINEERING

Journal of Engineering

journal homepage: www.jcoeng.edu.iq
Number 7 Volume 24 July 2018

Civil and Architectural Engineering

Finite Element Modeling and Parametric Study on Floor Steel Beam Concrete Slab System in Non-Composite Action.

Salah R. Al-Zaidee*
Lecturer
College of Engineering - University of Baghdad
salahalzaidee2004@gmail.com

Ehab Ghazi Al-Hasany
Researcher
College of Engineering - University of Baghdad
ehab0086@yahoo.com

ABSTRACT

This study aims to show, the strength of steel beam-concrete slab system without using shear connectors (known as a non-composite action), where the effect of the friction force between the concrete slab and the steel beam has been investigated, by using finite element simulation.
The proposed finite element model has been verified based on comparison with an experimental work. Then, the model was adopted to study the system strength with a different steel beam and concrete slab profile. ABAQUS has been adopted in the preparation of all numerical models for this study.
After validation of the numerical models, a parametric study was conducted, with linear and non-linear Regression analysis. An equation regarding the concrete slab-steel beam system strength in non-composite action has been pointed out. Where the actual strength of the beam without using shear connectors has been located in between the full composite action and non-composite action. However, partial-composite action has been noted, due to the effectiveness of friction force which makes the beam behave as composite before the slip occurs.
Keywords: steel beam floor system, non-composite action, finite element analysis, dimension analysis, regression analysis.

دراسة قوة نظام العتب الفولاذي والسقف الكونكريتي بطريقة العناصر المحددة في حالة التصرف بطريقة غير مركبة

د.صلاح رحيمة الزيدي
مدرس
كلية الهندسة – جامعة بغداد

إيهاب غازي خميس
بـاحث
كلية الهندسة – جامعة بغداد

الخلاصة

تهدف هذة الدراسة الى تقدير قوة نظام العتب الفولاذي مع السقف الكوكنريتي في حالة التصرف بطريقة غير مركبة اي في حالة عدم استعمال وصولات قص لغرض الربط بينهما، حيث تم البحث في مدى تأثير قوى الأحتكاك المتولدة بين السقف الكونكريتي والعتب الفولاذي، وتم ذلك عبر محاكاة الواقع بواسطة طريقة العناصر المحددة.
تم التـأكد من صحة تصرف النموذج المعد بواسطة العناصر المحددة عبر مقارنة النتائج العددية مع النتائج العملية وبعد ذلك تم اعتماد النموذج لغرض معرفة قوة النظام المستخدم حيث تم الأعتماد على برنامج ال ABAQUS عند إعداد النماذج العددية.

*Corresponding author
Peer review under the responsibility of University of Baghdad.
https://doi.org/10.31026/j.eng.2018.07.07

Article accepted: 12/10/2017

بعد التأكد من صحة النماذج العددية والتي اعدت مع الأخذ بنظر الاعتبار تأثير قوى الاحتكاك المتولدة بين السقف الكونكريتي والعتب الفولاذي، تم اجراء دراسة إحصائية وتحليل خطي ولاخطي بواسطة برنامج الSPSS لغرض الحصول على معادلة تبين مدى قوة نظام السقف الكونكريتي مع العتب الفولاذي المستخدم.

الكلمات الرئيسية: نظام أرضية العتب الفولاذي، التصرف بطريقة غير مركبة، التحليل بواسطة العناصر المحددة، التحليلات البعدية.

1. INTRODUCTION

In steel beam floor system, the members that are oriented perpendicular to the span of the slab system are usually referred to as beams, and the members that support the beams and are oriented parallel to the span of the slab system are usually called girders as shown in **Fig. 1** In this floor system, the headed studs are usually used to engage the concrete slab with the steel beams, in that case, the system is designed as a composite system. By contrast, if the headed studs are not used the beams are treated as a non-composite **Abi Aghayere, Jason Vigil, 2009**.

Adopting of partial composite action for the slab and the supporting floor beams without using shear connectors seem natural from the economical point of view to prepare a competitive design and from theoretical point of view where sophisticated finite element software have almost transformed these enhanced simulations from a state of art to state of practice.

2. REVIEW OF LITERATURE

Composite action is developed when two load-carrying structural members such as a concrete floor system and the supporting steel beam are integrally connected and deflect as a single unit as in **Fig. 2b**. The extent to which composite action is developed depends on the provisions made to ensure a single linear strain from the top of the concrete slab to the bottom of the steel section. The non-composite beam of **Fig. 2a**, wherein if friction between the slab and beam is neglected, the beam and slab each carry separately a part of the load. This is further shown in **Fig. 3**. When the slab deforms under vertical load, its lower surface is in tension and elongates, while the upper surface of the beam is in compression and shortens. Thus, a discontinuity will occur at the plane of contact. Since friction is neglected, only vertical internal forces act between the slab and beam **Salmon, et al., 2009**.

When beam system acts compositely **Fig. 3b** and **c** no relative slip occurs between the slab and beam. Horizontal forces (shears) are developed that act on the lower surface of the slab to compress and shorten it, while simultaneously they act on the upper surface of the beam to elongate it, **Salmon, et al., 2009**.

By an examination of the strain distribution that occurs when there is no interaction with the concrete slab bottom surface and the top flange of steel beam as shown in **Fig. 3a**, the overall resisting moment is:

$$\Sigma M = M_{slab} + M_{beam} \quad (1)$$

It is noted that in this case, there are two neutral axes: one at the slab center of gravity and the other one is at the beam center of gravity. The horizontal slip resulting from the bottom of the slab in tension and the top of the beam in compression is also indicated **Salmon, et al., 2009**.

When only partial interaction is presented, is shown in **Fig. 3b.** The slab neutral axis is closer to the beam and the beam neutral axis is closer to the slab. Due to the partial interaction, the horizontal slip has now decreased. The result of the partial interaction is the partial development

of the maximum compressive and tensile forces C' and T', in the concrete slab and steel beam respectively. Then the resisting moment of the section increased by the amount of T'e' or C'e'.

When complete interaction (known as a full composite action) between the slab and the beam is developed, no slip occurs and the resulting strain diagram is shown in **Fig. 3c**. Under this condition, a single neutral axis occurs which lies below that of the slab and above that of the beam. In addition, the compressive and tensile forces C" and T", respectively, are larger than the C' and T' existing with partial interaction. The resisting moment of the fully developed composite section then becomes

$$\Sigma M = T"e" \ \ or \ C"e" \tag{2}$$

However, even if shear connectors are not used, the partial composite action is expected in the initial stage of loading, as **Koskie, 2008** study indicates that "*there is an unintended partial composite action between steel stringer and concrete slab built without mechanical shear connectors. The non-composite bridges have been found to exhibit partial composite action at service loads, but at larger loads, the degree of composite action can decline resulting in the floor system performing as a non-composite action*".

In this study, the effect of friction force between the concrete slab and the steel beam in the non-composite action were investigated, where a comparison between the three cases of non-composite action, partial-composite action, and full-composite action was presented.

3. VERIFICATION STUDY

The verification study has been done through comparing the reference finite element model that was adopted in this study with the work of **Al-Hasany and Al-Zaidee, 2017**, which presents an experimental study of steel beam-concrete slab system as shown in **Fig. 4** and **5**.

In their work, **Al-Hasany and Al-Zaidee, 2017** tested four specimens and studied the effectiveness of concrete slab in restraining lateral torsional buckling of steel beam, this study was including the overall strength of the steel beam-concrete slab system.

Characteristics for the steel parts adopted in **Al-Hasany and Al-Zaidee, 2017** study have been presented with referring to **Fig. 6** and Table 1 where the yielding stress was tested and found to be $Fy = 340$ MPa and 309 MPa for beam flange and web respectively.

The adopted concrete slab has an average compressive strength of 34.7MPa and has the following characteristics:

- Thickness and width are $t = 75\ mm$ and $w = 1500mm$ respectively.
- The concrete slab has been reinforced with steel rebar As indicated in below, having a yielding stress equal to $f_y = 415$ MPa.
  - Long direction: Ø10@300 top and bottom,
  - Short direction: Ø10@300 bottom,
  - Short direction: Ø10@100 top

3.1 Tests Setup

The specimens were loaded by applying a uniform distributed load. The specimens with a total length of 2.9 m were set up on a testing machine, two steel rods were provided to support the specimens at each corner. The load then was applied by a hydraulic jack. The test setup is shown in **Fig. 7**, and schematically in **Fig. 8**.

3.2 Tests Results

Test results showed that the concrete slab, in general, could prevent the lateral torsional buckling. The ultimate loads for these specimens are presented in Table 2.

In this paper, the reference model is based on the steel-concrete beam with rough top flange specimen.

4. FINITE ELEMENT VALIDATION

In this work, a three-dimensional finite element model was developed using ABAQUS software package.

The beam was modeled using shell element. Beam ends were simulated to be similar to the simple ends usually adopted in actual connection in the floor beam system by using steel angles to connect the beam-ends to the girders. The girders were supported in the bottom flange as shown in **Fig. 9**.

The concrete slab was modeled by using shell element sitting in the steel beam top flange. The load was applied to the slab top surface to investigate the non-composite beam strength as shown in **Fig. 10**.

In ABAQUS, reinforcement bars are included in the "host" elements (concrete elements) using the REBAR option. The option is used to define layers of uniaxial reinforcement in the membrane, shell, and solid elements. Such layers are treated as a smeared layer with a constant thickness equal to the area of each reinforcing bar divided by the reinforcing bar spacing. **Fig. 11** shows the reinforcement bars embedded in shell elements as presented in ABAQUS.

ABAQUS provides more than one approach for defining contact. In this study, the contact between the slab bottom surface and the beam top flange was defined by using the contact pairs approach as it can provide a better interaction control. When a contact pair contains two surfaces, the two surfaces are not allowed to include any of the same nodes and one must choose which surface will be the slave and which will be the master, the finite-sliding, surface-to-surface formulation is used by default in this approach. The default contact pressure-overclosure relationship used by ABAQUS is referred to as the "hard" contact model, which has been adopted in this work. For the tangential behavior, and by default, ABAQUS assumes that contact between surfaces is frictionless. But it can include a friction model as part of a surface interaction definition, which has been adopted in this study by assigning the coefficient of friction of 0.6 between the concrete slab and the steel beam **Vayas and Iliopoulos, 2014**.

4.1 Materials Modeling

4.1.1 Structural Steel

In ABAQUS software, when modeling plastic materials, the Cauchy stress and the logarithmic plastic strain are used. the material properties in the tensile coupon test are computed from nominal-stress (σ), and engineering strain (ε), thus it is needed to be converted to true stress (σ_{true}) and plastic true strain (ε_{true}^{pl}) using the following relations **Kim, 2015**.

$$\sigma_{true} = \sigma(1+\varepsilon) \quad (3)$$

$$\varepsilon_{true}^{pl} = \ln(1+\varepsilon) - \sigma_{true}/E_o \quad (4)$$

where E_o is the initial Young's modulus σ and ε are respectively the measured nominal (engineering) stress and strain values. The initial part of the stress-strain curve from origin to the proportional limit stress can be represented based on the linear elastic model as given in

ABAQUS. The nonlinear part of the curve passed the proportional limit stress can be represented based on classical plasticity model as given in ABAQUS. The model allows to input a nonlinear curve by giving tabular values of stresses and strains. When performing an elastic-plastic analysis at finite strains, ABAQUS assumed that the elastic strains are small and the plastic strains control the deformation **Ellobody, 2014**.

In this paper and based on **Al-Hasany and Al-Zaidee, 2017** work, the adopted material property for steel are as indicated below:

$E_o = 200{,}000\ MPa$ $F_Y = 309\ MPa$ $F_u = 425\ MPa$

4.1.2 Concrete

Mainly, there are two material modeling approaches for concrete in ABAQUS, which are concrete smeared cracking and concrete damaged plasticity. Both models can be used to model plain and reinforced concrete.

In this paper concrete smeared crack has been adopted, where the concrete smeared cracking model is designed as a model of concrete behavior for relatively monotonic loadings under low confining pressures, that is less than 4-5 × the magnitude of the largest stress which the concrete can carry in the uniaxial compression; **Fig. 12**, **SIMULIA/ABAQUS, 2013**.

The most important feature of the behavior is assumed to be the cracking. The behavior representation of cracking and post-cracking dominates the modeling. The cracking is assumed to take place when the stress reaches the failure surface, that is called the crack detection surface.

In this paper and based on **Al-Hasany & Al-Zaidee, 2017** work, the adopted material property for concrete are $E_o = 24{,}500\ MPa$ and $f_{cu} = 34.7\ MPa$ for elastic modulus and compressive strength respectively.

4.2 Results

To simulate the actual steel beam behavior in the finite element model, a yield stress $F_y = 216\ MPa$ has been adopted. This yield stress has been reduced by 30% to account for the effect of residual stress **Segui, 2013**.

The model behavior of the steel beam-concrete slab system showed a good agreement with the experimental work. **Fig. 13** shows an agreement between experimental and numerical load-displacement curves.

5. PARAMETRIC STUDY

5.1 Steel Concrete Beam Behavior

As stated earlier the strength of the steel beam-concrete slab system in non-composite action is

$$\Sigma M = M_{slab} + M_{beam}$$
$$M_{non-composite} = A_s f_{y_{slab}} \left(d - {}^{a}/_{2}\right) + F_{y_{beam}}\, Z_x \qquad (5)$$

where

A_s is the area of the slab tension reinforcement, $f_{y_{slab}}$ is the yielding stress of the slab reinforcement, d is the slab effective depth, $F_{y_{beam}}$ is the yielding stress of the steel beam, Z_x is the plastic section modulus.

In this study, the following moment resisting has been pointed out;

$M_{slab} = 6.3.\ kN.m$

$M_{beam} = 22.5\ \ kN.m$

The total moment strength

$$\Sigma M = 6.3 + 22.5 = 28.8\ kN.m$$

The strength of the steel-concrete beam in full-composite action and based on calculations presented in Table 3 would be

$$M_{composite} = 49.7\ kN.m$$

Table 4 shows a comparison between the system moment strength in full-composite, non-composite and when the friction force included in the finite element model.

The results shown in

Table 4 indicates that the strength of the steel-concrete beam without using shear connectors, was between the full composite action and non-composite action, i.e. the partial-composite action is appeared due to the effectiveness of friction force which will make the beam behave as composite before the slip occurs.

5.2 Dimensional Analysis

Dimensional analysis is a method usually adopted to reduce the number and complexity of variables that affect a given physical phenomenon through using a sort of compacting technique. If a phenomenon depends on *n*-dimensional variables, the dimensional analysis will reduce the problem to only *k* dimensionless variables, where the reduction $n - k$ =1, 2, 3, or 4, depending on the problem complexity. Generally $n - k$ equals the number of different dimensions (sometimes called basic, primary, or fundamental dimensions) that govern the problem **White, 2011**.

There are several methods of reducing the number of dimensional variables into a smaller number of dimensionless groups. The scheme adopted here was proposed in 1914 by **Buckingham, 1914** and is now called the "*Buckingham Pi Theorem*" The name pi comes from the mathematical notation π, meaning a product of variables. The dimensionless groups found from the theorem are power products denoted by π_1, π_2, π_3, etc. The method allows the pi groups to be found in sequential order without resorting to free exponents **White, 2011**.

The pi theorem first part explains what reduction in variables to expect: "*If a physical process satisfies the principle of dimensional homogeneity (PDH) and involves n dimensional variables, it can be reduced to a relation between only k dimensionless variables or π_s. The reduction $j = n - k$ equals the maximum number of variables that do not form a pi among themselves and is always less than or equal to the number of dimensions describing the variables*" **White, 2011**.

The second part of the theorem shows how to find the pi groups one at a time: "*Find the reduction j, then select j scaling variables that do not form a pi among themselves.* Langhaar, 1951, *Each desired pi group will be a power product of these j variables plus one additional variable, which is assigned any convenient nonzero exponent. Each pi group thus found is independent*" **White, 2011**.

The beams moment strength was obtained as a function of the steel-concrete beam in non-composite action.

As recommended by **Salmon, et al., 2009** when there is no interaction between the concrete slab and the steel beam and since friction is neglected, it is seen that the total resisting moment is equal to

$$\Sigma M_{non-composite} = M_{slab} + M_{beam}$$

$$M_{non-composite} = A_s f_{y_{slab}} \left(d - {}^{a}/_{2}\right) + F_{y_{beam}} Z_x$$

As stated earlier when the friction force is included, the beam will behave as a partial composite. The actual moment strength can be written as follow:

$$M_{partial} = f\{M_{non}, \mu\} \quad (6)$$

$$M_{partial} = f\{A_s, f_{y\,slab}, d, a, F_{y\,beam}, Z_x, \mu\} \quad (7)$$

where μ is the coefficient of friction.

Since the required form of the moment strength is to be as a function of the non-composite action, the above equation can be written as

$$\frac{M_{partial}}{M_{non-composite}} = f\{A_s, f_{y\,slab}, d, a, F_{y\,beam}, Z_x, \mu\} \quad (8)$$

The effect of all variables in the partial composite strength was investigated by using finite element analysis.

Table 5 **5** shows the variables and dimensions that was included in the dimensional analysis.

- number of variables n = 8
- number of dimensions $j = 2$
- number of dimensionless groups $\pi_s = 8 - 2 = 6$

Let the repeating variables $F_{y_{slab}}, d$ which cannot be combined into a pi group, thus:

$$\pi_1 = M_{partioal}/M_{non-composite} \quad (9)$$

$$\pi_2 = (F_y)^a (d)^b A_s \quad (10)$$

$$N^0 m^0 = (N\,m^{-2})^a (m)^b m^2$$

$a = 0, b = -2$, thus

$$\pi_2 = \frac{A_s}{d^2}$$

From the same procedure:

$$\pi_3 = \frac{a}{d} \quad (11)$$

$$\pi_4 = \frac{F_{y\,beam}}{f_{y\,slab}} \quad (12)$$

$$\pi_4 = \frac{F_{y\,beam}}{f_{y\,slab}} \quad (13)$$

$$\pi_6 = \mu \quad (14)$$

The relationship between the pi groups can be written as

$$\pi_1 = f\{\pi_2, \pi_3, \dots, \pi_6\} \quad (15)$$

$$\frac{M_{partioal}}{M_{non-composite}} = f\left\{\frac{F_{y\,beam}}{f_{y\,slab}}, \frac{Z_x}{d^3}, \frac{A_s}{d^2}, \frac{a}{d}, \mu\right\} \quad (16)$$

This is a complex six-variable function, but dimensional analysis alone cannot take further **White, 2011**. A number of finite element analysis were conducted to point out $M_{partial}$ values

with different beam and slab characteristics as shown in **Table 6**. After that, a regression analysis was undertaken to assemble all variables with the best equation.

5.3 Regression Analysis

The use of sample data to investigate the relations among a group of variables, ultimately to create a model for some variable that can be used to predict its value in the future. The process of finding a mathematical model (an equation) that best fits the data is part of a statistical technique known as regression analysis **Mendenhall and Sincich, 2012**.

Regression analysis is a branch of statistical methodology concerned with relating a response y to a set of independent, or predictor, variables $x_1, x_2, \ldots, x_k$. The goal is to build a good model, a prediction equation relating y to the independent variables that will be able to predict y for given values of and to do so with a small error of prediction. When using the model to predict y for a particular set of values, the reliability of our prediction must be measured. That is, it will be wanted to know how large the error of prediction might be. All these elements are parts of a regression analysis, and the resulting prediction equation is often called a regression model **Mendenhall and Sincich, 2012**.

In this work, an SPSS software was adopted to conduct the regression analysis, where SPSS Statistics is a software package used for logical batched and non-batched statistical analysis.

Firstly, linear regression analysis has been conducted, where the obtained equation has an R^2 value of (0.78). However, to improve the R^2 value, a non-linear regression analysis was undertaken after processing a curve estimation analysis for all variables separately with SPSS to improve the data with beast fitting.

From the non-linear regression analysis, the obtained equation is presented below with R^2 value of (0.995).

$$\pi_1 = 11.74 - (52.44\,\pi_2) + (-355.8\,\pi_3 + 2909\,\pi_3^2) - (0.622\,\pi_4) + (20.91\,\pi_5 - 27.7\,\pi_5^2) + (0.282\pi_6) \quad (17)$$

6. RESULTS AND CONCLUSIONS

The results indicate that the actual strength of the steel beam-concrete slab system without using shear connectors, was between the full composite action and non-composite action, i.e. the partial-composite action is appeared due to the effectiveness of friction force which will make the beam behave as composite before the slip occurs.

This study and based on the regression analysis, pointed out an equation of the steel beam-concrete slab system strength in non-composite action with frictional force effect included, as follow:

$$M_p/M_n = 11.74 - \left(52.44\,\frac{A_s}{d^2}\right) + \left(-355.8\,\frac{a}{d} + 2909\,\left(\frac{a}{d}\right)^2\right) - \left(0.622\,\frac{F_{y\,beam}}{f_{y\,slab}}\right) + \left(20.91\,\frac{Z_x}{d^3} - 27.7\left(\frac{Z_x}{d^3}\right)^2\right) + (0.282\,\mu)$$

7. REFERENCES

- Abi Aghayere, Jason Vigil, 2009. *Structural Steel Design.* New Jersey: Pearson Prentice Hall, pp. 269-271.
- Al-Hasany, Ehab G, and Al-Zaidee, Salah R., 2017. *Effectiveness of Slabs in Restraining Lateral Torsional Buckling of Steel Floor beams.* Baghdad: International Journal of Science and Research (IJSR).
- Buckingham, E., 1914. *On Physically Similar Systems: Illustrations of the Use of Dimensional Equations*.
- Ellobody, Ehab., 2014. *Finite Element Analysis and Design of Steel-Concrete Composite Bridges.* Tanta University, Egypt: Elsevier Inc.. p. 502.
- Kim, Nam-Ho., 2015. *Introduction to Nonlinear Finite Element Analysis.* New York: Springer Science+Business Media New York. p. 351.
- Koskie, Jeremy Craig. 2008. *Investigation of steel stringer bridge superstructures.* Iowa: s.n. p. 17.
- Langhaar, H. L., 1951. *Dimensional Analysis and the Theory of Models.* New York: Wiley.
- Mendenhall, William, and Sincich, Terry., 2012. *REGRESSION ANALYSIS.* 7. Boston: Pearson Education, Inc.. pp. 81-89.
- Salmon, Charles G., Johnson, John E. and Malhas, Faris A., 2009. *STEEL STRUCTURES DESIGN AND BEHAVIOR.* 5. United States of America: Person Education, Inc. pp. 806-808.
- Segui, William., 2013. *STEEL DESIGN.* 5. United States of America: Global Engineering. p. 204.
- SIMULIA/ABAQUS., 2013. *Analysis User's Manual.* United States of America: ABAQUS INC.
- White, Frank M., 2011. *Fluid Mechanics.* 7. New York: McGraw-Hill. pp. 293-304.

8. NOMENCLATURE

A_s =	area of the slab tension reinforcement, mm^2.
b =	steel beam width, mm.
C' =	maximum compressive force in partial-composite action, kN.
d =	slab effective depth, mm.
e =	the distance between resultant tension and compressive force, mm.
E_o =	initial Young's modulus, MPa.
Fy=	yielding stress, MPa.
F_u=	ultimate stress, MPa.

f_{cu}= concrete cube compressive strength, MPa.
h = steel beam depth, mm.
j= number of dimensions, No.
M_{beam}= steel beam moment strength, kN.m.
$M_{composite}$= beam strength in full-composite action, kN.m.
$M_{non-composite}$ = beam strength in non-composite action, kN.m.
$M_{partial}$= beam strength in partial-composite action, kN.m.
M_{slab}= concrete slab moment strength, kN.m.
n= number of variables, No.
M_{slab}= concrete slab moment strength, kN.m.
T'= maximum tension force in partial-composite action, kN.
t = slab thickness, mm.
t_f = flange thickness, mm.
t_w = web thickness, mm.
w= slab width, mm.
Z_x.= plastic section modulus, mm^3.
σ= nominal-stress, MPa.
σ_{true} = true stress, MPa.
ε = engineering strain, dimensionless.
ε_{true}^{pl} = plastic true strain, dimensionless.
μ = the coefficient of friction, dimensionless.
π_s= number of dimensionless groups, No.

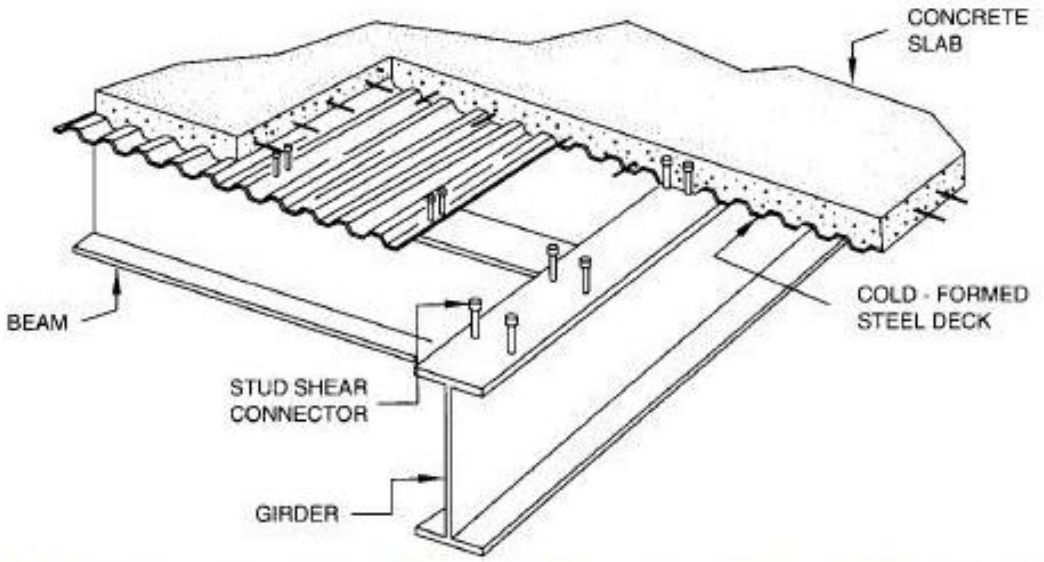

Figure 1. Steel beam floor system**.**

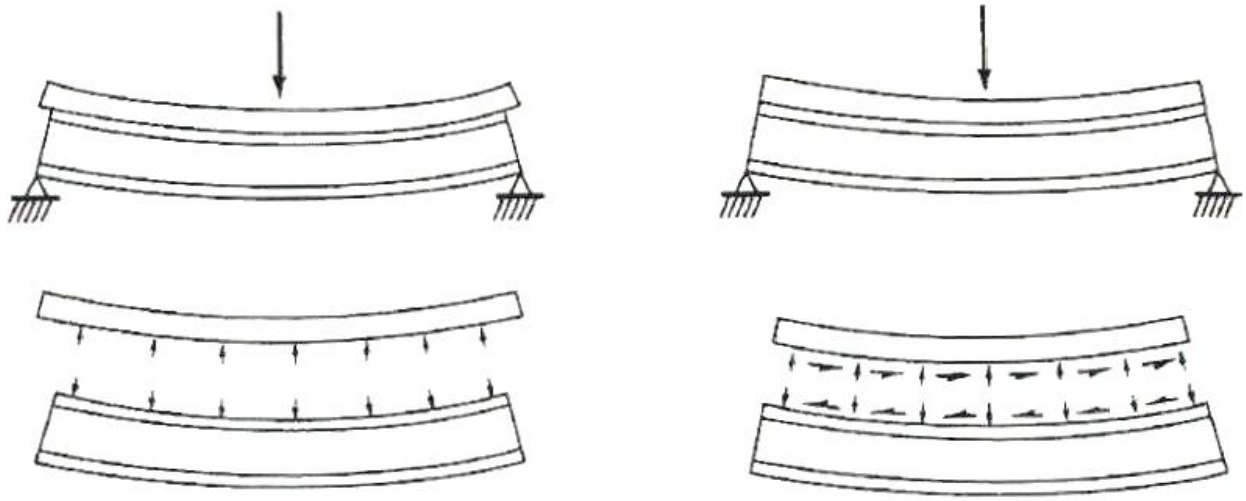

Figure 2. Composite and non-composite action**.**

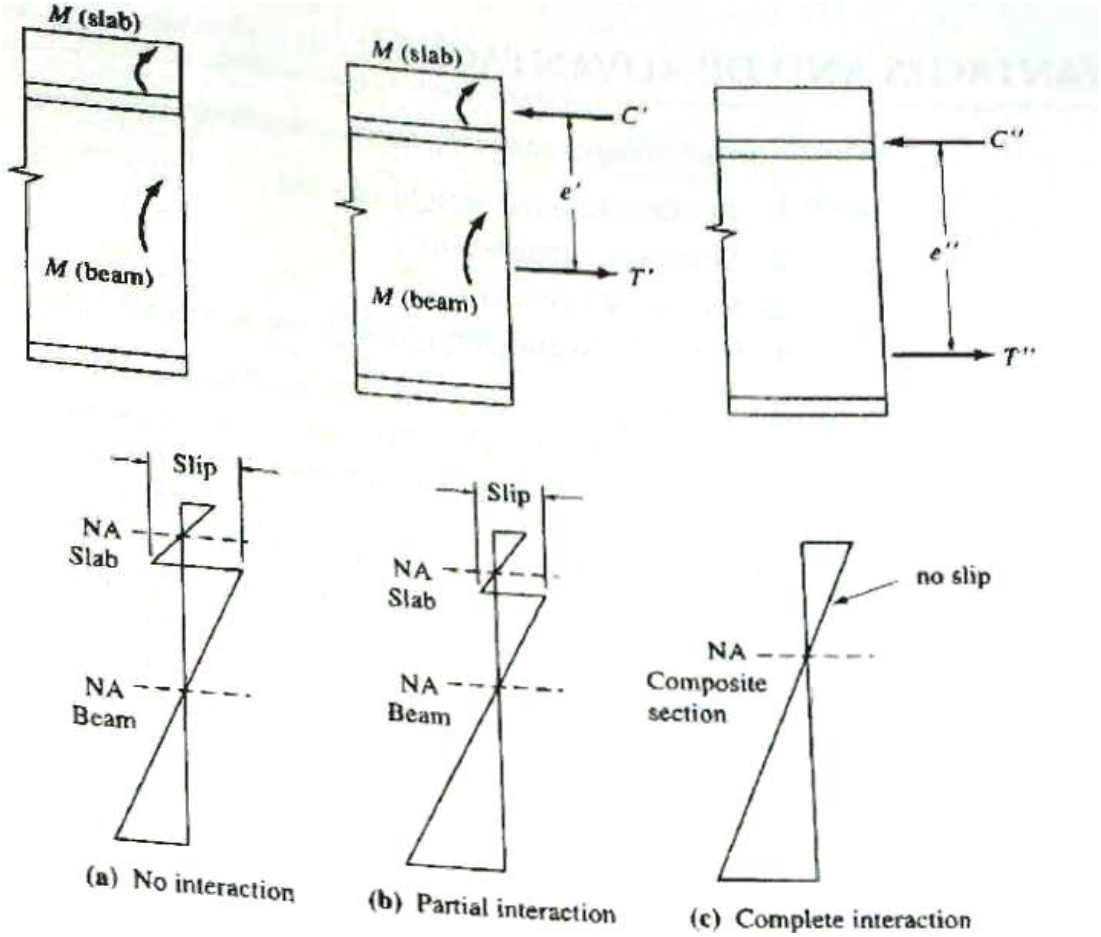

Figure 3. Strain variation in composite beams.

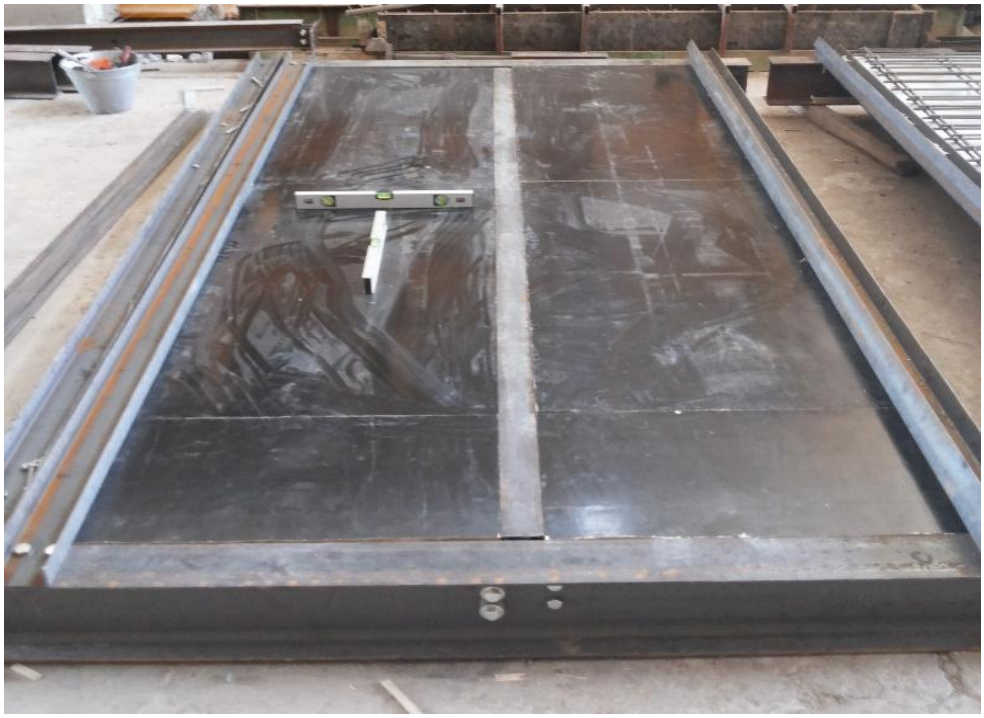

Figure 4. Steel beam-concrete slab system.

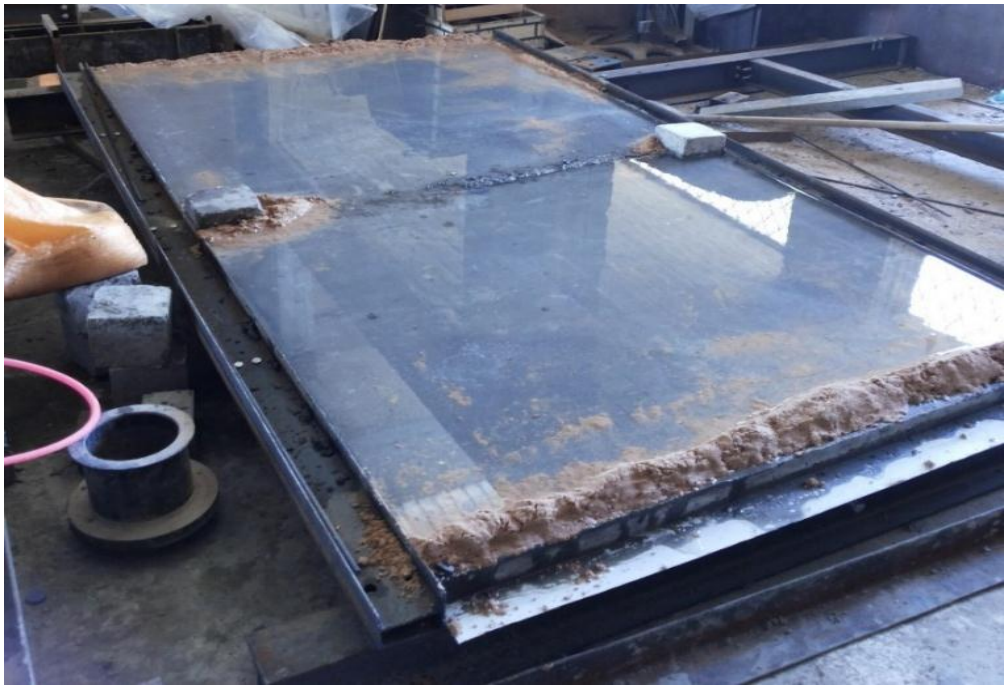

Figure 5. Steel beam-concrete slab system continued.

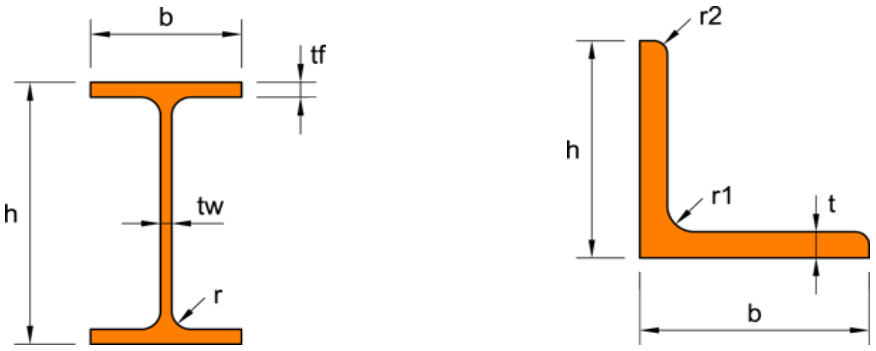

Figure 6. Reference dimensions for the adopted steel section.

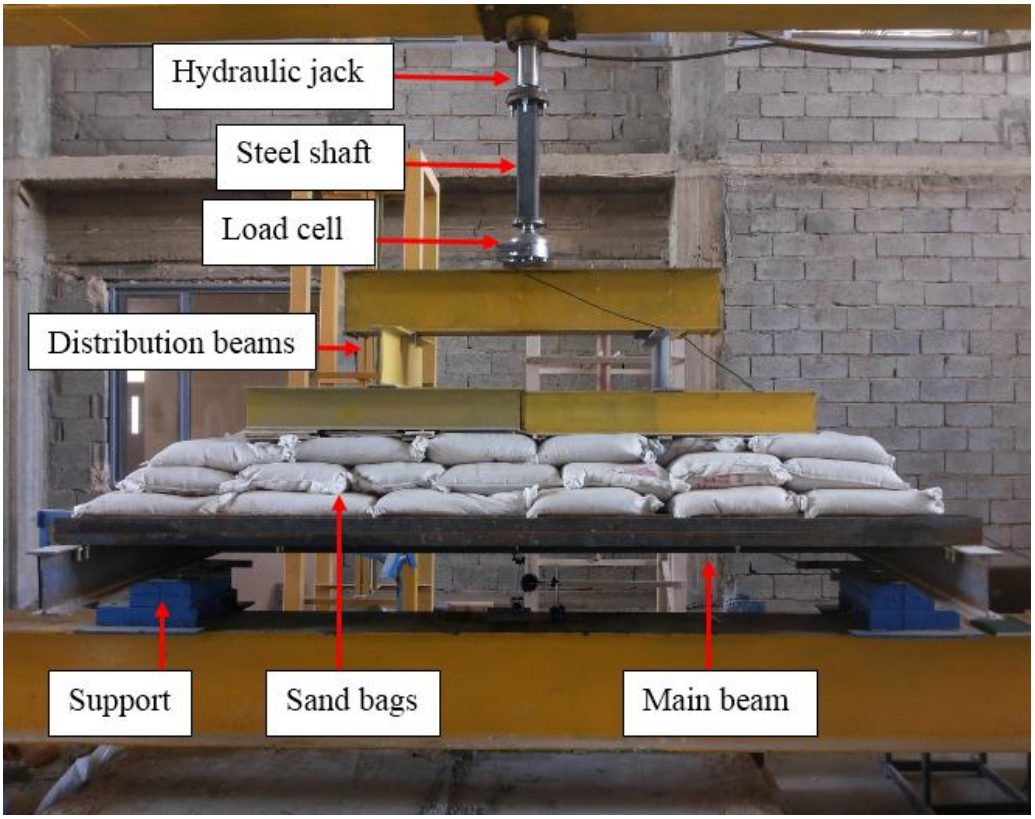

Figure 7. Test setup.

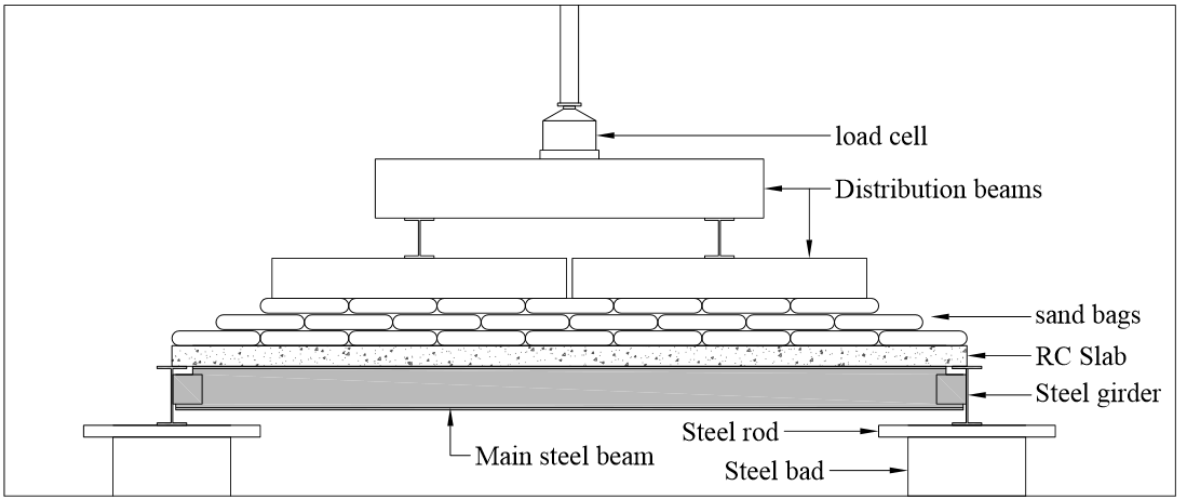

Figure 8. Schematic drawing of the test setup.

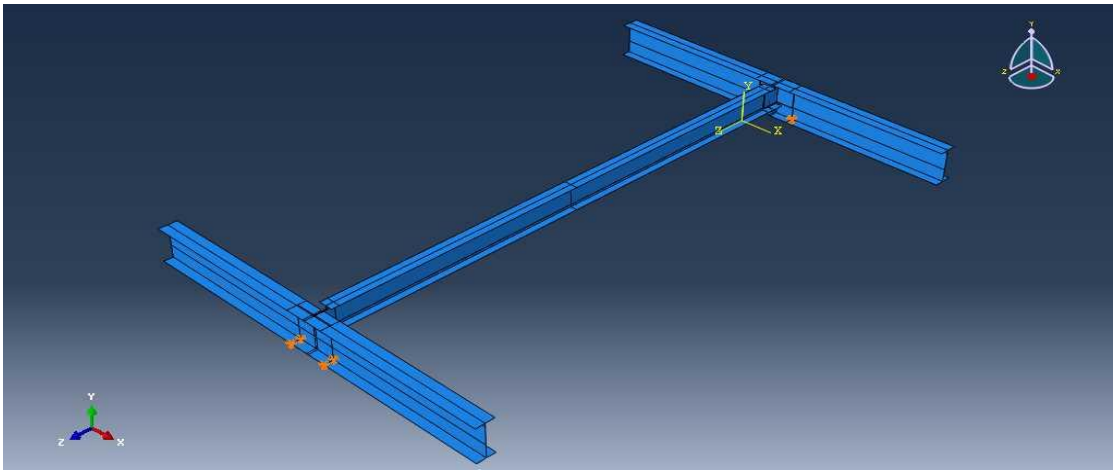

Figure 9. Boundary conditions.

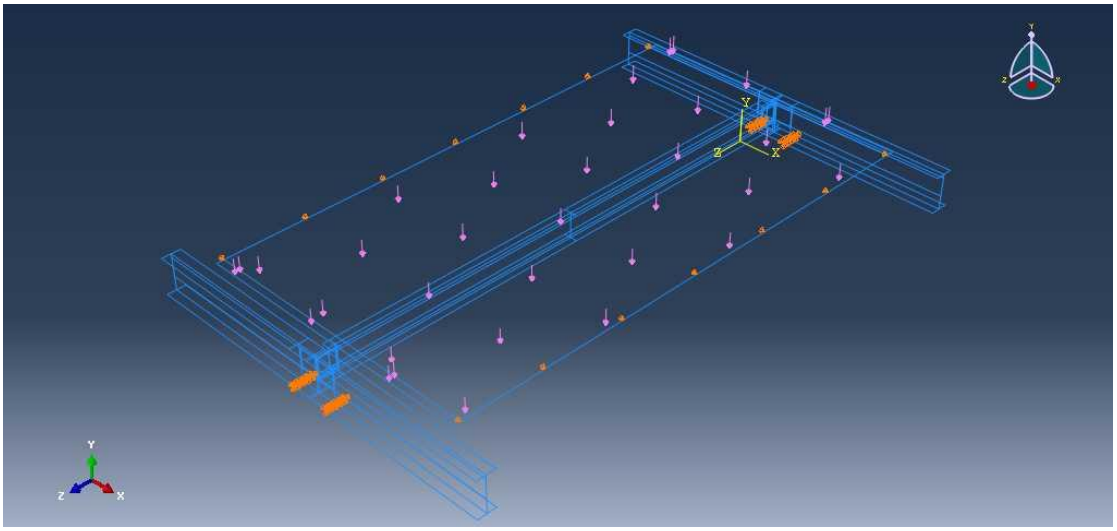

Figure 10. Steel-concrete beam simulation for rough and smooth top flange.

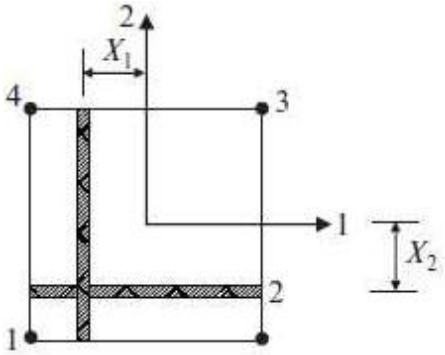

Figure 11. Rebar location in a 3D shell or membrane element as presented in ABAQUS.

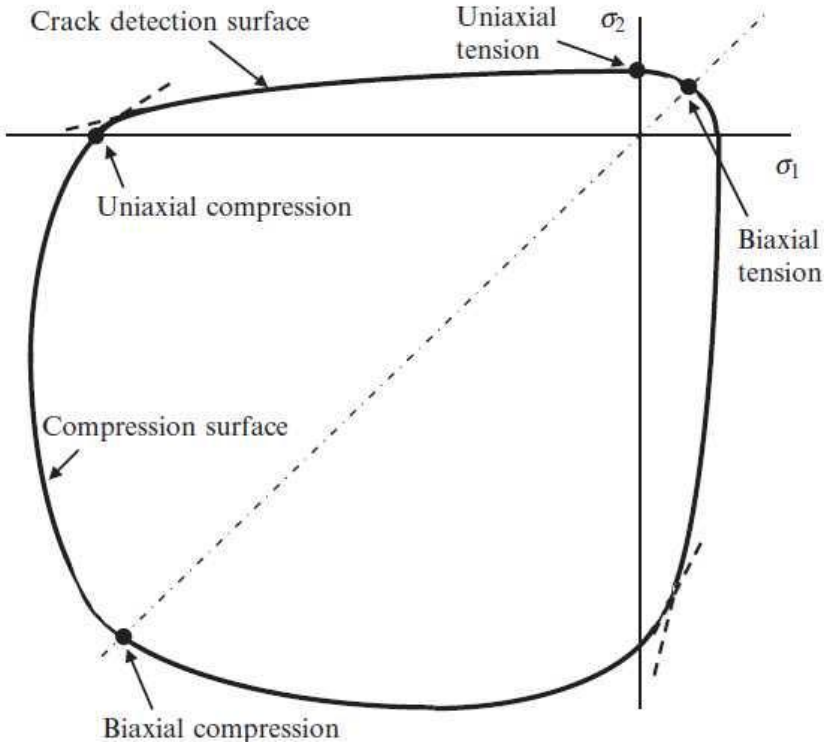

Figure 12. Yield and failure surface in plane stress as given in ABAQUS.

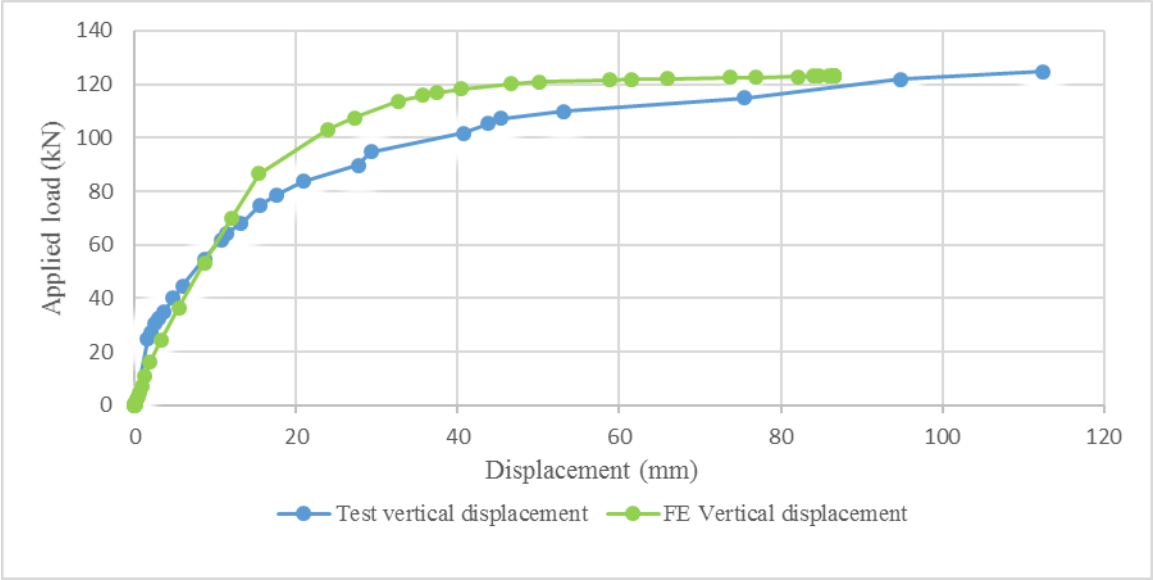

Figure 13. Experimental and FE load-displacement curves for a steel-concrete beam with a rough top flange.

Table 1. Steel Parts detail (all dimensions are in mm)**.**

PART	h	b	t_f	t_w	Length
MAIN BEAM, IPE140	142	75	8	6	2900
GIRDER, IPE220	200	99	8	5.5	2000
ANGLE	100	100	5		100
BOLTS	16				

Table 2. Failure loads.

#	***Model type***	***Failure load (kN)***
2	Steel-concrete beam (rough top flange)	124.78
3	Steel-concrete beam (smooth top flange)	109.04
4	Steel-concrete beam with Corrugated metal deck	119.78

Table 3. Calculation sheet for the full composite action.

Full composite section design							
I beam			**Concrete slab**				
bf=	75	mm	beff=	350	mm		
h=	142	mm	tc=	75	mm	Concrete thickness above th	
tf=	8	mm	hr=	0	mm	Deck thickness (height of th	
tw=	6	mm	Ac=	26250	mm2		
A=	1956	mm2	fc'=	25	Mpa		
ho=	134	mm	E=	23650	Mpa		
E =	200000	Mpa	n=	8.4566596			
Fy=	216.3	Mpa	Act=	3104.0625	mm2		
Lb=	2700	mm	Ix=	1455029.3	mm4		
Iy=	564768	mm4	**Composite Beam**				
Ix=	6393388	mm4	yslab=	37.5			
Sx= Ix/(h/2)	90047.71831	mm3	ybeam=	146			
J =(2bf tf^3 +ho tw^3)/3	35248	mm4	Ayslab=	116402.34			
G=	77200	Mpa	Aybeam=	285576			
ry=√ Iy/A	16.9922393	mm	y'composite=	79.441379	mm	from top	
c=	1		dslab=	-41.94138			
Zx= $b_f\ t_f\ (h-t_f)+0.25\ t_w(h-2t_f)^2$	104214	mm3	dbeam=	66.558621			
Cw=$\frac{Iy\ ho^2}{4}$	2535243552	mm6	**I**composite=	21973887	mm4		
Full Composite							
THE PNA within the concrete slab							
$C = 0.85f'_cA_c$	557812.5	Mpa					
$C = F_yA_s$	423082.8	Mpa					
C =	423082.8	Mpa					
$C = 0.85f'_cab$	a= 56.88508235						
$M_n = A_sF_y\left(\frac{d}{2}+h_r+t_c-\frac{a}{2}\right)$	49736538.8	N.mm					
	49.7365388	kN.m					

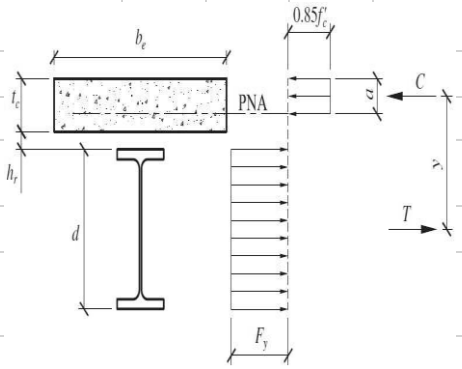

Table 4. Steel-concrete beam flexure strength.

Analysis type	***Failure moment kN.m***
Full composite action	49.7
Non-composite action	28.8
Beam of the present study	42.7

Table 5. variables and dimensions

Variables / Units	M_p/M_n	A_s	$f_{y_{slab}}$	d	a	$F_{y_{beam}}$	Z_x	μ
N	0	0	1	0	0	1	0	0
m	0	2	-2	1	1	-2	3	0

Table 6. Groups characteristics

	Groupe 1	Groupe 2	Groupe 3	Groupe 4	Groupe 5	Groupe 6	Groupe 7	Groupe 8	Groupe 9
Beam characteristics									
bf =	75	75	75	75	75	75	75	75	64
tf =	8	8	8	8	8	8	8	6	6
h =	142	142	142	142	142	142	142	142	132
tw =	6	6	6	6	6	6	6	4.5	4
Zx=	104214	104214	104214	104214	104214	104214	104214	80212.5	62784
fy beam=	216	300	340	216	216	216	216	216	216
μ =	0.6	0.6	0.6	0.4	0.1	0.6	0.6	0.6	0.6
Slab characteristics									
b =	1000	1000	1000	1000	1000	1000	1000	1000	1000
d =	60	60	60	60	60	60	85	60	60
As=	261.9	261.9	261.9	261.9	261.9	196.425	261.9	261.9	261.9
fc =	27.2	27.2	27.2	27.2	27.2	27.2	27.2	27.2	27.2
Fy slab =	420	420	420	420	420	420	420	420	420
$a = (A_s F_y)/(0.85 f_c b)$	4.757699	4.757699	4.757699	4.757699	4.757699	3.5682742	4.757699	4.757699	4.757699
Resultes									
$P_{failure}$ =	44.28	51.3	56.07	42.12	39.6507	42	54.24	43.08	31.98
$M_{partioal}$ =	42776694	49558365	54166424	40690026	38304559	40574100	52398552	41617434	30894279
$M_{Non-composite}$ =	28848435	37602411	41770971	28848435	28848435	27312945	31598385	23664111	19899555
$\pi_1 = M_p/M_n$	1.4828081	1.3179571	1.296748	1.410476	1.3277864	1.4855263	1.6582668	1.758673	1.552511
$\pi_2 = A_s/d^2$	0.07275	0.07275	0.07275	0.07275	0.07275	0.0545625	0.0362491	0.07275	0.07275
$\pi_3 = a/d$	0.079295	0.079295	0.079295	0.079295	0.079295	0.0594712	0.0559729	0.079295	0.079295
$\pi_4 = F_{y\,beam}/f_{y\,slab}$	0.5142857	0.7142857	0.8095238	0.5142857	0.5142857	0.5142857	0.5142857	0.5142857	0.5142857
$\pi_5 = Z_x/d^3$	0.4824722	0.4824722	0.4824722	0.4824722	0.4824722	0.4824722	0.1696951	0.3713542	0.2906667
$\pi_6 = \mu$	0.6	0.6	0.6	0.4	0.1	0.6	0.6	0.6	0.6